Article:
Dew, L., English, W.R., Ortega, I. et al. (2016) Fabrication of biodegradable synthetic vascular networks and their use as a model of angiogenesis. Cells Tissues Organs. 446644. ISSN: 1422-6405

https://doi.org/10.1159/000446644

Fabrication of biodegradable synthetic vascular networks and their use as a model of angiogenesis

Lindsey Dew, William R English[a], Ilida Ortega[b], Frederik Claeyssens[*], Sheila MacNeil[*]

Kroto Research Institute, University of Sheffield, Broad Lane, Sheffield S3 7HQ, UK. [a]Tumour Microcirculation Group, Department of Oncology, School of Medicine, The University of Sheffield, Sheffield, S10 2RX, UK. [b]School of Clinical Dentistry, Claremont Crescent, University of Sheffield, Sheffield S10 2TA, UK.

Short Title: Synthetic vascular nets as 3D models of angiogenesis

Keywords: Angiogenesis, Electrospinning, Robocasting, Tissue Engineering, Regenerative Medicine.

*Corresponding Author:

Kroto Research Institute, University of Sheffield, Broad Lane, Sheffield S3 7HQ, UK. Dr Frederik Claeysens (Email: f.claeyssens@sheffield.ac.uk, Tel: +44 (0) 114 222 5513, Fax: +44 (0) 114 222 5943) & Professor Sheila MacNeil (Email: s.macneil@sheffield.ac.uk, Tel: +44 (0) 114 222 5995, Fax: +44 (0) 114 222 5943)

Abstract

One of the greatest challenges currently faced in tissue engineering is the incorporation of vascular networks within tissue-engineered constructs. The aim of this study was to develop a technique for producing a perfusable, three-dimensional cell friendly model of vascular structures that could be used to study the factors affecting angiogenesis and vascular biology in engineered systems in more detail. Initially, biodegradable synthetic pseudo-vascular networks were produced via the combination of robocasting and electrospinning techniques. The internal surfaces of the vascular channels were then recellularized with human dermal microvascular endothelial cells (HDMECs) with and without the presence of human dermal fibroblasts (HDFs) on the outer surface of the scaffold. After 7 days in culture, channels that had been reseeded with HDMECs alone, demonstrated irregular cell coverage. However when using a co-culture of HDMECs inside and HDFs outside the vascular channels, coverage was found to be continuous throughout the internal channel. Using this cell combination, collagen gels loaded with vascular endothelial growth factor were deposited onto the outer surface of the scaffold and cultured for a further 7 days after which endothelial cell (EC) outgrowth from within the channels into the collagen gel was observed showing the engineered vasculature maintains its capacity for angiogenesis. Furthermore the HDMECs appeared to have formed perfusable tubules within the gel. These results show promising steps towards the development of an *in vitro* platform upon which to study angiogenesis and vascular biology in a tissue-engineering context.

Introduction

There has been significant progress in the field of tissue engineering over recent years, however one of the current obstacles blocking major clinical translation is the production of thick (≥2 mm), complex tissues due to the lack of rapid neovascularization of the constructs [Griffith et al., 2005]. Blood vessel formation is tightly regulated and relies on the chronologically precise adjustment of vessel growth, maturation and suppression of EC growth - all of which are controlled by a large number of factors that influence each other [Carmeliet and Jain, 2011]. To induce vascularization within tissue engineered (TE) substitutes these same processes need to occur and it is therefore not surprising that this remains a challenge in the tissue-engineering field.

The most promising approaches to circumvent slow revascularization of tissue engineered constructs have historically used the body as an in vivo bioreactor making use of the omentum and in some case arteriovenous shunts. For example Baumert et al 2007 and Saxena et al, 2010 used the omentum and the body as an *in vivo* bioreactor for tissue engineering of bladder and cardiac tissue respectively. Baumert et al used pig urothelial and smooth muscle cells seeded into sphere shaped small intestinal submucosa (SIS) matrix grafts and after 3 weeks, transferred into the omentum in the pig. Three weeks later at harvest, these were found to be highly vascularised and the authors concluded that the omentum permitted the *in vivo* maturation of these seeded scaffolds with the development of a dense vasculature which they anticipate to prevent fibrosis and loss of contractility. Saxena et al implanted their tissue engineered constructs - ovine oesophageal epithelial cells implanted on collagen sheets pre-seeded with fibroblasts to form a rudimentary

tubularised oesophagus into the sheep omentum and demonstrated vascular coverage and ingrowth into the periphery of the construct.

An alternative approach is that of using an arteriovenous shunt. Burla et al 2005 achieved vascularisation for neonatal cardiac myocytes placed in silicone chambers close to a vascular pedicle. In 2006 Kneser et al used an arteriovenous loop in a rat model to overcome the problem of engineering larger volume bone tissues. This approach of using an AV shunt was considered in a review of the challenges of angiogenesis and tissue engineering by Laschke et al 2006. These authors concluded however that future directions should focus on the creation of microvascular networks within 3D tissue constructs *in vitro* prior to implantation. We have also recently reviewed this area (Dew et al., 2015 and conclude that progress remains slow in neovascularisation of tissue engineered constructs because there are very few systems which allow one to study perfusion conditions, the cell type and scaffold architecture – all of which are important for neovascularization. We suggest it is therefore important to take a step back and understand how these factors work together to promote angiogenesis in order to advance this crucial area.

Clinically the study of angiogenesis has increased rapidly over the last 40 years as a result of its major role in a number of pathologies including cancer, rheumatoid arthritis and retinopathies to name but a few [Carmeliet, 2000]. Assays have been developed in an attempt to study the process. Ideally these would enable the assessment of multiple factors, providing reliable and reproducible results directly relating to those found in the clinic [Staton et al., 2009]. From the observations gleaned from tissue engineering strategies this would include the combination of a relevant vascular architecture, the ability to incorporate the relevant cell combinations

along with flow conditions and appropriate extracellular matrix (ECM) components. There is currently no single ‘gold standard' assay that provides a useful platform to incorporate all of these elements in an *in vitro* setting.

We have developed a novel 4-step technique to produce an *in vitro* angiogenesis model via the combination of electrospinning and robocasting methods used widely in the tissue-engineering field [Ortega et al., 2015]. Using the combination of these two approaches offers a range of advantages in the design of angiogenesis assays. For instance, the use of robocasting allows for the tuning of the vascular network geometry in terms of size, thickness and morphology enabling bespoke designs to be tested rapidly and scaled-up easily where necessary. The use of electrospun fibres provides high levels of porosity and surface area to enable diffusion and facilitate cell attachment, respectively [Ashammakhi et al., 2008]. In addition electrospinning also offers the ability to easily spin different polymers allowing for the control of degradation times [Blackwood et al., 2008] and mechanical properties whilst enabling the combination of different membrane combinations, as recently reported by our group [Bye et al., 2013]. Synthetic pseudovascular networks produced via this methodology provide a surface that supports EC adhesion [Ellis-Behnke et al., 2006; Beachley and Wen, 2010; Bye et al., 2013] and could provide the ability to test a range of angiogenic growth factors, combine multiple cell combinations and study the effects of perfusion through interconnected afferent and efferent channels. In this study we firstly describe the recellularization of such scaffolds using both HDMECs and HDFs in different combinations. We then describe the use of these scaffolds to observe the outgrowth of 3D tubular structures into a Vascular Endothelial Growth Factor (VEGF) loaded collagen gel.

125

126 **Materials and Methods**

127 *Production of synthetic pseudovascular nets.* Synthetic pseudovascular nets were
128 produced using a 4 step technique using a combination of electrospinning and
129 robocasting as previously published [Ortega et al., 2015]. Briefly, electrospun mats
130 were produced by dissolving medical grade poly(3-hydroxybutyrate-co-3-
131 hydroxyvalerate) (PHBV; Goodfellow) in a mixture of dichloromethane (DCM) and
132 methanol. An optimal concentration of 10% w//w of PHBV (containing 10% w//w of
133 methanol) was prepared and electrospun. Alginate was robocast onto the PHBV
134 electrospun mat with the purpose of acting as a sacrificial template. An alginate paste
135 was placed inside a syringe barrel attached to a dispensing system (Ultra 2800, EFD
136 Inc., East Province, USA) whilst a 3D printer (RepRap Mendel, Oldbury on Severn,
137 UK) was used to hold the dispensing arm and print the alginate. The electrospinning
138 process was then repeated to cover the alginate sacrificial template with a nanofibrous
139 PHBV layer. To remove the alginate and achieve the creation of a hollow network
140 between the two electrospun mats, the scaffolds were submerged in 0.5 M
141 ethylenediaminetetraacetic acid (EDTA) solution overnight on a gel-shaker set to 70
142 rpm.
143 The overall dimensions of these nets as shown in Fig 1 were 2x4cm with tubes that
144 were approximately 0.5 mm wide with a flat bottom and curved ceiling with a height
145 of 0.15 mm (please see [Ortega et al., 2015] for detailed structures). The hexagonal
146 section of the scaffold measured approximately 5x7.5mm at the widest points.
147

148 *Cells and cell culture* Proliferating HDMECs from juvenile foreskin (Promocell,
149 Heidelberg, Germany) were grown in gelatin coated (0.1% (w/v) pig skin gelatin in

PBS) T25 tissue culture flasks. Cells were grown in EC growth medium MV containing 0.05ml/ml FCS, 0.004 ml/ml EC growth supplement, 10ng/ml epidermal growth factor (recombinant human), 90 μg/ml heparin, 1 μg/ml hydrocortisone, 100 U/ml penicillin, 0.1 mg/ml streptomycin and 0.25 μg/ml amphotericin B. Media was replenished every 2-3 days. HDMECs were passaged when they reached approximately 80% confluence, split using a ratio of 1:3 and were used at passage 5 in this study. HDFs were cultured from skin samples taken from consenting patients undergoing elective abdominoplasty or breast reduction surgery, as described previously [Bye et al., 2014] and used under the requirements stipulated by Research Tissue Bank Licence 12179. HDFs were cultured in DMEM supplemented with FCS (10% v/v), streptomycin (0.1 mg/ml), penicillin (100 IU/ml) and amphotericin B (0.5 g/ml) and used between passage 6-8.

Endothelialization of synthetic pseudovascular nets. Prior to cell culture, scaffolds were sterilized by immersion into 70% ethanol (v/v in distilled water) for 30 minutes, followed by washing with sterile PBS. Scaffolds were then cannulated with a 24G cannula (BD Insyte™) under a dissection microscope (Wild Heerbrugg M3Z). In this study, varying cell combinations were seeded onto and within the synthetic scaffolds. These included; HDMECs seeded into the channels, a combination of HDMECs and HDFs seeded within the channels and finally HDMECs seeded within the channels and HDFs seeded on the outside surface of the channels. To ensure cells attached uniformly to the artificial channels seeding was performed using a two-stage process. First, 0.5×10^6 HDMECs (per scaffold) were resuspended in 0.25ml of EC growth medium MV. Using a 1ml syringe the cell suspension was injected into the scaffold through the cannula, submerged in media and kept overnight in an incubator at 37 °C

and 5% CO_2. The constructs were then turned over and a second suspension of 0.5×10^6 HDMECs was seeded and left overnight. For the introduction of HDFs into the channels, HDMECs were firstly allowed to attach to the scaffolds for a minimum of 3 hours before injecting 0.5×10^6 HDFs and repeating this process following the second injection of HDMECs. For the introduction of HDFs onto the outside surface of the channels 0.5×10^6 HDFs were pipetted over the outer surface of the scaffolds immediately after the seeding of the HDMECs. The scaffolds were placed in an incubator for up to 2 hours at 37 °C and 5% CO_2 without being submerged in media to allow attachment of the HDFs. The scaffolds were then subsequently submerged in media overnight before repeating the process.

Outgrowth of endothelial cells from biodegradable scaffolds into an extracellular matrix. Scaffolds that had been recellularized and cultured at 37°C and 5% CO_2 for 7 days were taken and the channels were pierced with a sterile 21G hypodermic needle (Terumo, MediSupplies, UK) to introduce small holes into the scaffold to allow cell migration out of the scaffold. Collagen gels (2 mg/ml) were prepared by adding 200 μl rat tail collagen type I (3 mg/ml, Gibco, Life technologies, UK) to 100 μl of concentrated MEM solution (Gibco, Life Technologies, UK) and vascular endothelial growth factor (VEGF) to a final concentration of 10 ng/ml. The collagen solution (~50 μl) was then pipetted into the wells formed by the channels and allowed to set at 37°C for 15 min. The scaffolds were then submerged in media and cultured for a further 7 days, changing the media every 3 days.

Immunohistochemistry Samples were fixed for 2 hours in 4% paraformaldehyde (PFA) w/v in HBSS with Ca^{2+} and Mg^{2+} before dehydrating using graded alcohol

washes and embedding in paraffin wax. 6 μm sections were cut and mounted on slides and stained with Hematoxylin and Eosin (H&E) (Sigma Aldrich).

Immunofluorescence staining. Immunofluorescence staining was performed as described previously [Correa de Sampaio et al., 2012]. Briefly, samples were fixed in 4% PFA (w/v) in HBSS with Ca^{2+} and Mg^{2+} for 30 minutes. Samples were then quenched with 100 mM glycine, washed once with PBS and then blocked for 1 h with 1% (w/v) bovine serum albumin (BSA) in PBS at room temperature (RT). Separate samples were then incubated with mouse monoclonal anti-human CD31 (1:20 in 1% (w/v) BSA, Dako, UK) and mouse monoclonal anti-human VE cadherin (CD144) (1:50 in 1% (w/v) BSA, BD Biosciences) at RT overnight.. The scaffolds were subsequently washed for 2 h in 1% BSA (w/v) in PBS with 0.1% Tween (v/v), followed by incubation with Alexa Fluor™ 546 nm goat anti-mouse secondary antibody (1:200 in 1% (w/v) BSA) (Life technologies) for 2 h at RT before counterstaining with the nuclear stain DAPI (1:1000 in 1% (w/v) BSA). Finally the scaffolds were washed with 1% BSA (w/v) in PBS with 1% Tween (v/v) for at least 8 h, after which the samples were imaged using a Zeiss LSM 510 confocal microscope (Zeiss, UK) to observe cellular organization.

Perfusion with FITC-lectin To visualize potential vessel formation, the scaffolds were perfused with 100 μl of FITC labelled tomato lectin (Vector Laboratories) at a rate of 40 μl/min, controlled using a syringe pump (Genie Plus, Kent Scientific, Connecticut, USA).The scaffolds were then fixed in 4% PFA (w/v) in HBSS with Ca^{2+} and Mg^{2+} for 30 minutes and subsequently immunostained for CD31 as described above.

Results

The formation of a continuous endothelial cell monolayer within the pseudovascular net lumen requires the support of fibroblasts

In order for the electrospun pseudovascular net (shown in Fig 1A) to act as a model vascular structure that can support neovascularization within biological structures, optimization of seeding and growth of an endothelial monolayer within the scaffold lumen was performed. Initially HDMEC were injected (by perfusing the nets by inserting a syringe as shown in Fig 1B) at high density within the lumen alone and allowed to adhere to the upper and lower surfaces. After 7 days culture cell coverage was investigated using hematoxylin and eosin staining of the pseudovascular net in cross-section (Fig 2). Although HDMEC could be detected, coverage was not continuous (Fig. 2 A –C). Mesenchymal cells, including pericytes and fibroblasts, have been shown to support endothelial function in *in vitro* models, mimicking perivascular cells [Kirkpatrick et al., 2011]. To determine if HDFs can augment HDMEC adhesion and survival within the pseudovascular net, HDFs were first seeded within the lumen with the HDMECs as in other vascular models this can result in a self-organising system replicating endothelial-pericyte architecture [Kunz-Schughart et al., 2006; Hurley et al., 2010]. This resulted in continuous cellular coverage of the inside of the lumen (Fig. 2 D-F). As some of the signalling pathways known to regulate endothelial barrier function are also soluble growth factors, we also seeded HDFs on the outside of the pseudovascular net and HDMECs on the inside of the lumen, physically separating the cells. On H&E staining, increased cell coverage of the lumen was seen, although this did not appear as continuous as the seeding both HDMECs and HDFs within the lumen (Fig 2 G-I).

To further characterize the EC coverage within the lumen of the pseudovascular net, the net was sectioned to reveal the upper curved surface and the lower flat surface before staining with CD31 and DAPI and confocal imaging. In nets seeded with HDMECs alone, CD31 staining lacked continuity and the ECs had a rounded appearance, with little to no evidence of CD31 at cell-cell junctions, especially on the curved surface (Fig 3 A-B). Although H&E staining showed a continuous cell layer with both HDFs and HDMECs were seeded within the lumen, the CD31 staining did not show continuous endothelial coverage. However, unlike surfaces with ECs alone, patches of confluent ECs were observed with discernable cell-cell junction staining of CD31 that appeared to be partially detracted from the HDFs cells on the pseudovacular net, suggesting poor adhesion (Fig 3 C-D). In contrast, the combination of HDFs on the external surface and HDMECs on the internal surface generated a continuous endothelial monolayer with a characteristic 'cobblestone' appearance and clear cell-cell junction staining of CD31, particularly on the curved surface (Fig 3 E-F). Furthermore, staining for the endothelial adherens junction protein VE-Cadherin confirmed the establishment of a confluent monolayer on the inside of the lumen when HDFs were cultured on the outside (Fig 4 A-B).

Endothelial cells maintain the capacity to migrate out of the pseudovascular net to form new perfusable vascular structures within a biological matrix

After establishing the HDMECs could form a continuous monolayer of cell within the lumen of the pseudovascular net, we next aimed to determine if these had the capacity to form new vascular structures within a biological matrix, as this would be required if the artificial vascular structure is to have the ability to integrate with engineered tissues or biological material in the future. Initial studies indicated that

HDMECs would not be able degrade the electrospun mat or invade through it in a timely manner for this to occur. Accordingly, the pseudovascular net was punctured providing discreet exit points for the HDMECs. The well-shaped region within the net's hexagon pattern was then filled with collagen-I gel containing VEGF to promote migration of the ECs from within the net into the gel (Fig 5A). After 7 days of culture a CD31 positive network was found extending throughout this collagen-I gel with the appearance of a crude vascular network (Fig 5B) surrounded by HDFs that had also migrated into the gel.

We then aimed to determine if the new vasculature could be perfused via the pseudovascular net by injection of FITC-Lectin, commonly used *in vivo* to investigate vascular function [Thurston et al., 1998; Ezaki et al., 2001; Mazzetti et al., 2004]. Confocal imaging showed significant overlap between CD31 and FITC-Lectin indicating perfusion had occurred (Fig 5C). It is important to note that these experiments were repeated 5 times with at least 6 replicates per experiment and vessel formation was found in around 50% of samples.

These structures generated in the pseudovascular nets were apparently random and looked more like large sinusoids/lymphoid structures than blood vessels. In width they ranged from 10μm up to structures which at their widest were closer to 80μm. There was no obvious pattern. They extended partially throughout the collagen /VEGF gel (spanning approximately 1cm from the peripheral vascular channel in all directions) within the 7 days of culture.

Discussion

The aim of this study was to develop a controllable 3D *in vitro* model of vascular structures to study the factors affecting angiogenesis and vascular biology. The

ultimate aim of this work is to translate the use of such vascular networks to the clinic in order to assist in the "take" of TE materials that lack intrinsic vasculature.

For many years it has been recognized that while it is possible to produce human 3D TE constructs in the laboratory, unless they are very thin epithelial structures they can be lost upon transplantation due to delays in neovascularization [Griffith et al., 2005]. Introducing a vascular network into a TE construct is a major challenge which only a few groups are tackling. In an attempt to understand the fundamental principles behind the induction of angiogenesis, development of 3D models investigating the interactions between different cell types have progressed [Montesano et al. 1993; Donovan et al., 2001; Santos et al., 2008]. Other studies have looked at the influence of fluid flow on EC survival and sprouting [Moll et al., 2013; Vukadinovic-Nikolic et al., 2014]. However, we are unaware of any models that have the ability to combine different cell combinations and fluid flow to investigate the induction of early stage blood vessel formation for TE applications.

This work represents a significant step towards this goal. Our aim was to develop a simple synthetic pseudo-vascular network which could be recellularized to form an interconnected monolayer of ECs. A promising or successful structure was viewed as one which could demonstrate evidence of new vessel formation, sprouting outwardly from these re-endothelialized channels. The main finding of this study was the production of tubular architectures emerging from the pseudo-vasculature in response to the proangiogenic mitogen VEGF.

This study shows that lining of the synthetic vasculature with HDMECs was not very successful when these cells were introduced on their own. Their ability to adhere and form a continuous lining was much improved by the addition of HDFs, particularly when added to the outer layer of the synthetic channels. In summary endothelial

cover was relatively poor with HDMECs alone, better with the inclusion of HDFs inside the lumen together with HDMECs but best of all with HMDEC inside and HDFs outside the lumen. In other recent studies we show that fibroblasts themselves are not able to penetrate through a nanofibrous PHBV electrospun layer even after two weeks of culture [Bye et al., 2013 and 2014].

Accordingly we speculate that this arrangement, HDMECs inside the channels with HDFs outside, provides the opportunity for cross talk and "reassurance" of the HDMECs by the fibroblasts as found in other studies [Dietrich and Lelkes, 2006; Kunz-Schughart et al., 2006; Hughes, 2008; Kirkpatrick et al., 2011]. It is likely that both are producing soluble and ECM factors, however this was not investigated in this particular study.

After the successful re-endothelialization of the synthetic channels we were keen to explore whether new vessels would sprout from these channels in response to proangiogeneic stimuli; the criteria that had been originally selected as the definition of a successful system. Results showed that placing VEGF loaded collagen gels onto the scaffolds caused HDMEC outgrowth to occur from within the channels into the collagen gel showing that the engineered vasculature maintained its capacity for angiogenesis. Furthermore the HDMECs appeared to have formed perfusable tubules (determined by connecting these nets to a syringe pump and perfusing at 40 μl/min) within the gel. However, these tubules did not look like 'normal' blood vessels and were arguably closer to angiomas. There are many studies that show that VEGF on its own will direct migration of ECs but this commonly results in the formation of large and leaky vessels [Jain and Munn, 2000; Tomanek, 2002; Thurston, 2002]. It is suspected that this is the case in this particular study. It is also important to note that these results were found in around 50% of experiments, highlighting the need for

350 further optimization. However we emphasize that this is to the best of our knowledge
351 the first demonstration of endothelial tubule formation in 3D from a synthetic
352 vascular network. The rate of perfusion and detailed flow effects were not examined
353 in this study (perfusion was at a fixed rate of 40 μl/min in these experiments) but this
354 should now be possible using these synthetic pseudo-vascular networks. Similarly we
355 do not know what role the added fibroblasts play in the formation of these structures.
356 In summary we previously reported the production of an EC lined synthetic pseudo-
357 vascular network [Ortega et al., 2015]. This study has developed this work a
358 significant step further in showing the production of perfusable tubular sprouts
359 emanating from the HDMEC lined networks in response to the proangiogenic
360 mitogen VEGF. This system will now lend itself to investigations of perfusion flow,
361 the response of the cells to combinations of angiogenic mitogens and to the
362 examination of the nature of the cross talk between the HDMECs and HDFs. It will
363 also be important to examine the response to these cell-seeded constructs implanted in
364 an animal model in the future. Overall these results indicate promising steps towards
365 the development of an *in vitro* platform in which to study angiogenesis and vascular
366 biology for a range of applications.
367
368
369 **Acknowledgements**
370 We thank the EPSRC funded DTC Tissue Engineering and Regenerative Medicine
371 (EP/F505513/1) for support of LD and an EPSRC Landscape Fellowship
372 (EP/I017801/1) program for support of IO for this research.
373
374

List of Abbreviations

HDMECs	Human dermal microvascular endothelial cells
HDFs	Human dermal fibroblasts
EC	Endothelial cell
TE	Tissue engineered
ECM	Extra cellular matrix
VEGF	Vascular endothelial growth factor
PHBV	Poly(3-hydroxybutyrate-co-3-hydroxyvalerate)
DCM	Dichloromethane
EDTA	Ethylenediaminetetraacetic acid
H&E	Hematoxylin and Eosin
RT	Room temperature
PFA	Paraformaldehyde
FFPE	Formalin fixed paraffin embedded

400

401

402 **References**

403 Ashammakhi, N., et al (2008) Advancing tissue engineering by using electrospun
404 nanofibers. Regenerative medicine *3*: 547–74.

405 Baumert, H. et al (2007) Development of a seeded scaffold in the great omentum:
406 Feasiblity of an in vivo bioreactor for bladder tissue engineering. European
407 Urology *52*: 884-892.

408 Beachley, V., X. Wen (2010) Polymer nanofibrous structures: Fabrication,
409 biofunctionalization, and cell interactions. Progress in polymer science *35*: 868–
410 892.

411 Birla, R.K. et al (2005). Myocardial engineering in vivo: Formation and
412 characterization of contractile, vascularised three-dimensional cardiac tissue.
413 Tissue Engineering *11(5/6)*: 803-813

414 Blackwood, K.A., et al (2008) Development of biodegradable electrospun scaffolds
415 for dermal replacement. Biomaterials *29*: 3091–104.

416 Bye, F.J., et al (2013) Development of bilayer and trilayer nanofibrous/microfibrous
417 scaffolds for regenerative medicine. Biomaterials Science *1*: 942.

418 Bye, F.J., et al (2014) Development of a Basement Membrane Substitute Incorporated
419 Into an Electrospun Scaffold for 3D Skin Tissue Engineering. Journal of
420 Biomaterials and Tissue Engineering *4*: 686–692.

421 Carmeliet, P. (2000) Mechanisms of angiogenesis and arteriogenesis. Nature
422 Medicine *6:* 389–395.

423 Carmeliet, P., R.K. Jain (2011) Molecular mechanisms and clinical applications of
424 angiogenesis. Nature *473*: 298–307.

425 Correa de Sampaio, P., et al (2012) A heterogeneous in vitro three dimensional model
426 of tumour-stroma interactions regulating sprouting angiogenesis. PloS one 7:
427 30753.

428 Dew, L., S. MacNeil, et al (2015) Vascularization strategies for tissue engineers.
429 Regenerative medicine *10*: 211–24.

430 Dietrich, F., P. Lelkes (2006) Fine-tuning of a three-dimensional microcarrier-based
431 angiogenesis assay for the analysis of endothelial-mesenchymal cell co-cultures
432 in fibrin and collagen gels. Angiogenesis *9:* 111-25.

433 Donovan, D., et al (2001) Comparison of three in vitro human "angiogenesis" assays
434 with capillaries formed in vivo. Angiogenesis *4*: 113–121.

435 Ellis-Behnke, R.G., et al (2006) Nano neuro knitting: peptide nanofiber scaffold for
436 brain repair and axon regeneration with functional return of vision. Proceedings
437 of the National Academy of Sciences of the United States of America *103*:
438 5054–9.

439 Ezaki, T., et al (2001) Time course of endothelial cell proliferation and microvascular
440 remodeling in chronic inflammation. The American journal of pathology *158*:
441 2043–55.

442 Griffith, C.K., et al (2005) Diffusion limits of an in vitro thick prevascularized tissue.
443 Tissue Engineering *11:* 257–266.

444 Hughes, C. (2008) Endothelial–stromal interactions in angiogenesis. Current opinion
445 in hematology *3:*204-209.

446 Hurley, J.R., S. Balaji, et al (2010) Complex temporal regulation of capillary
447 morphogenesis by fibroblasts. American Journal of Physiology-Cell Physiology
448 *299*: 444–453.

449 Jain, R., L. Munn (2000) Leaky vessels? Call Angl1!. Nature medicine *6*:131–132.

450 Kirkpatrick, C.J., S. Fuchs, et al (2011) Co-culture systems for vascularization--
451 learning from nature. Advanced drug delivery reviews *63*: 291–9.

452 Kneser, U. et al (2006). Engineering of vascularized transplantable bone tissues:
453 Induction of axial vascularization in an osteoconductive matrix using an
454 arteriovenous loop. Tissue Engineering *12(7)*: 1721-1731.

455 Kunz-Schughart, L.A., et al (2006). Potential of fibroblasts to regulate the formation
456 of three-dimensional vessel-like structures from endothelial cells in vitro.
457 American journal of physiology *290:* 1385–98.

458 Laschke, M.W. et al (2006). Angiogenesis in tissue engineering: Breathing life into
459 constructed tissue substitutes. Tissue Engineering *12(8)*: 2093-2104.

460 Mazzetti, S., et al (2004) Lycopersicon esculentum lectin: an effective and versatile
461 endothelial marker of normal and tumoral blood vessels in the central nervous
462 system. European journal of histochemistry *48:* 423–428.

463 Moll, C., et al (2013). Tissue engineering of a human 3D in vitro tumor test system.
464 JoVE *78*.

465 Montesano, R., M. Pepper, et al (1993) Paracrine induction of angiogenesis in-vitro
466 by swiss 3T3 fibroblasts. Journal of cell science *105*: 1013–1024.

467 Ortega, I. et al (2015) Fabrication of biodegradable synthetic perfusable vascular
468 networks via a combination of electrospinning and robocasting. Biomater. Sci. *3*:
469 592–596.

470 Santos, M.I., et al (2008) Endothelial cell colonization and angiogenic potential of
471 combined nano- and micro-fibrous scaffolds for bone tissue engineering.
472 Biomaterials *29*: 4306–13.

473 Saxena, A.K. et al (2010). Esophagus tissue engineering: in situ generation of
474 rudimentary tubular vascularized esophageal conduit using the ovine model.
475 Journal of Paediatric Surgery *45*: 859-864.

476 Staton, C.A., M.W.R Reed, et al (2009) A critical analysis of current in vitro and in
477 vivo angiogenesis assays. International Journal of Experimental Pathology *90:*
478 195–221.

479 Thurston, G., et al (1998) Angiogenesis in mice with chronic airway inflammation:
480 strain-dependent differences. The American journal of pathology *153*:1099–112.

481 Thurston, G. (2002) Complementary actions of VEGF and angiopoietin-1 on blood
482 vessel growth and leakage. Journal of anatomy *200*:575–80.

483 Tomanek, R. (2002) Assembly of the vasculature and its regulation. Springer.

Vukadinovic-Nikolic, Z. et al (2014) Generation of Bioartificial Heart Tissue by Combining a Three-Dimensional Gel-Based Cardiac Construct with Decellularized Small Intestinal Submucosa. Tissue engineering part a *20*: 799–809.

Figure Legends

Figure 1. Appearance of pseudovascular net and diagram of its perfusion. **A** shows the appearance of one of the pseudovascular nets which had the overall dimensions of 2cm x 4cm. **B** shows that the pseudovascular net is designed to be cannulated with a needle and perfused. For detailed description of the production of the pseudovascular net, please see Ortega et al, 2015.

Figure 2. Immunohistochemical staining of human dermal fibroblasts and human dermal microvascular endothelial cells on the surfaces of the pseudovascular net

A – C. FFPE cross sections through a vascular scaffold where HDMECs were seeded on the inside of the scaffold lumen, stained with H&E and imaged 4, 10 and 20 × magnification respectively. (For a detailed description of the production of these scaffolds please see Ortega et al 2015).Scale bar shows 100 μM. **D – F**. As in A – C, but showing scaffolds with HDMECs and HDFs seeded within the scaffold lumen. **G – I.** As in A – C but with HDMECs seeded inside and HDFs seeded outside the vascular scaffold.

Figure 3. Confluent endothelial monolayers within the pseudovascular net's channels are formed with support of human dermal fibroblasts.

Pseudovascular nets were sectioned parallel to the lower surface of the channel (indicated by cartoon above images) and both surfaces were immunostained with anti-CD31 (HDMECs, red) and DAPI (nuclei, blue) before images were taken by confocal microscopy and z-stacked images compressed to generate an image of the whole surface. Scale bar = 100 μM. **A and B.** Upper and lower inner surfaces seeded with

HDMECs alone. **C and D.** Upper and lower inner surfaces seeded with HDMECs and HDFs seeded inside the channel of the vascular net. **E and F.** Upper and lower inner surfaces seeded with HDMECs inside the channel and HDFs seeded outside the channel of the pseudovascular net.

Figure 4. Endothelial cells on the inside surface of the pseudovascular net have VE-Cadherin positive adherens junctions. Pseudovascular nets were seeded with HDMECs inside the channel and HDFs outside the channels and sectioned as described in Fig 3. Sections were immunostained with anti-VE-Cadherin (red) and DAPI (nuclei, blue) before images were taken by confocal microscopy. Z-stacks of images were compressed to generate an image of the whole surface. **A** –Scale bar = 100 μM. **B** - Scale bar = 20 μM.

Figure 5. Human dermal endothelial cells exit the pseudovascular net to form a perfusable network within VEGFA loaded collagen-I gels. **A.** Diagram showing the process of making holes in a pseudovascular net that has been pre-seeded internally with HDMECs, and externally with HDFs. After 7 days culture, holes are made on the inner side of the net's artificial vascular channels facing into the hexagonal well using a 21 gauge needle. The hexagonal area is then filled with collagen-I containing VEGFA and allowed to set before submerging in medium for a further 7 days to allow growth of cells from the net into the collagen gel. **B.** 3D confocal projection of CD31 positive structures within the collagen-I gel from the centre of the hexagonal well. **C.** Confocal images of nuclei (blue), Lectin-FITC (green) and CD31 (red) and merged image of all three channels of the collagen-I gel within the centre of the hexagonal well after perfusion of the pseudovascular net with Lectin-FITC. Scale bar is 100 μm.

Figure 1

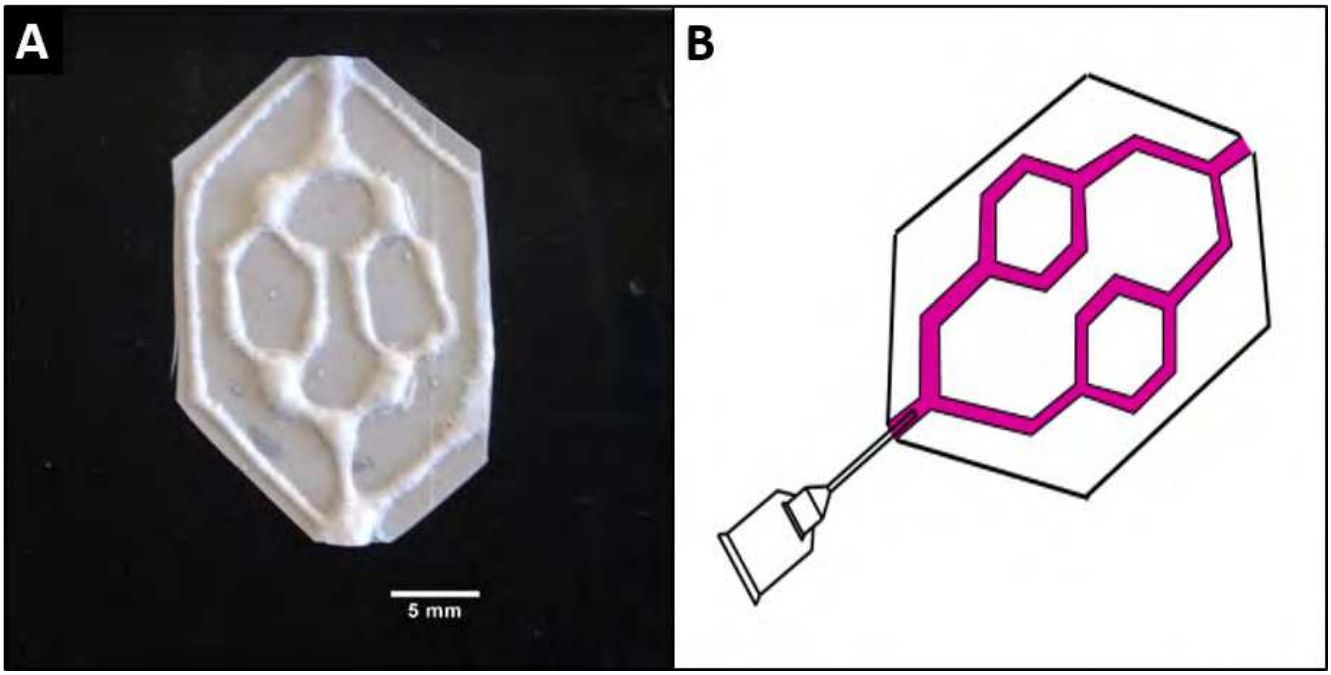

Figure 2

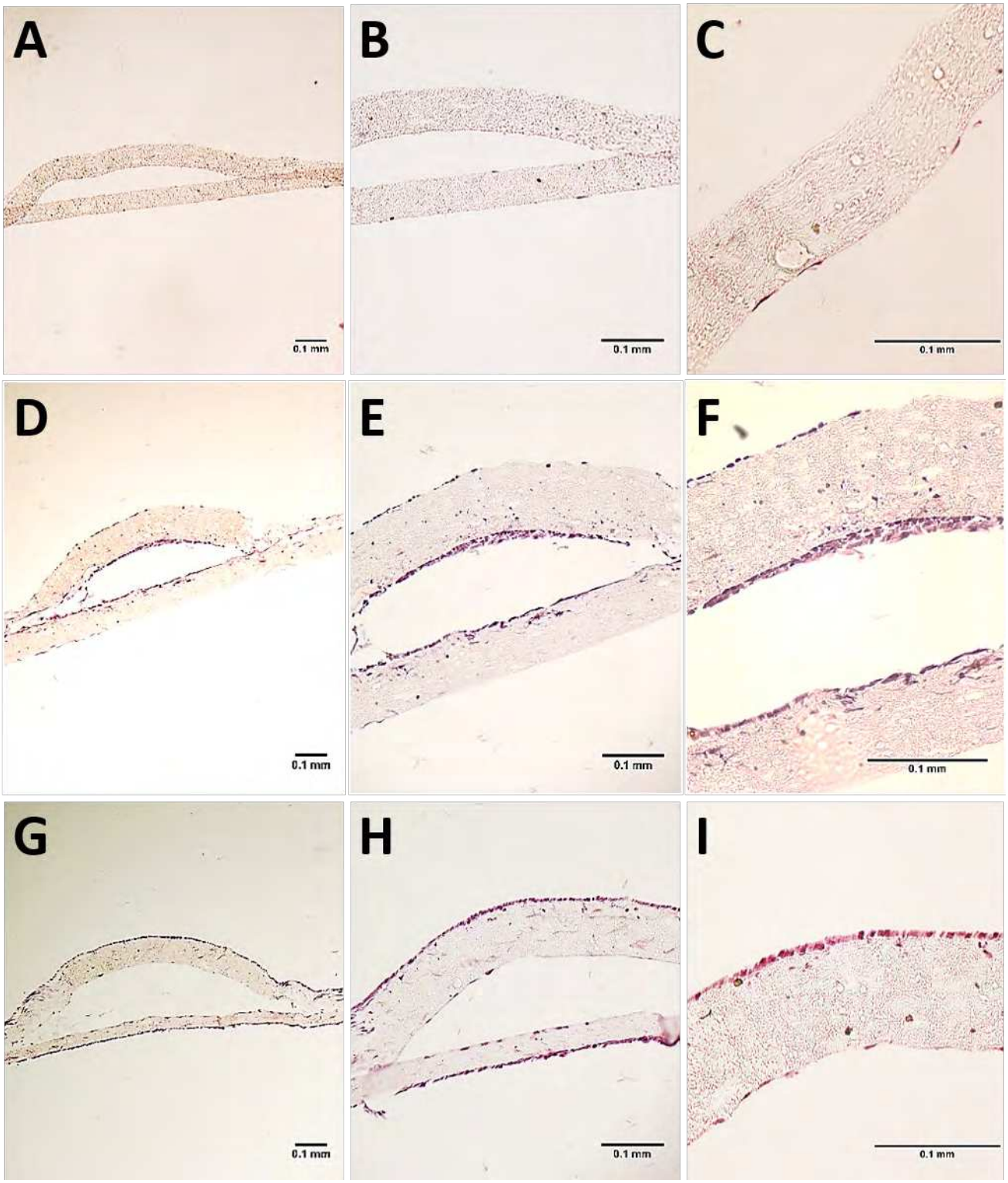

Figure 3

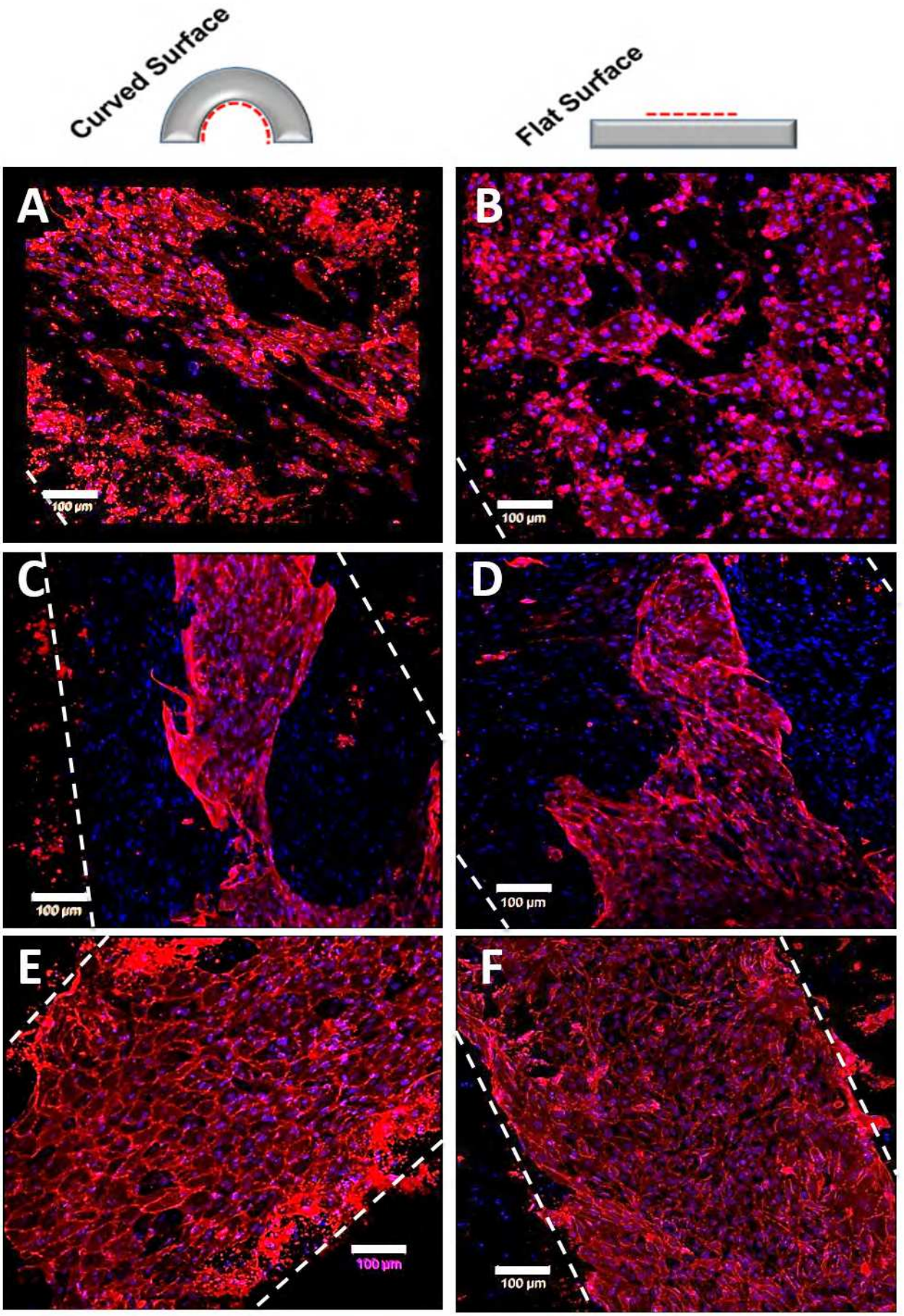

Figure 4

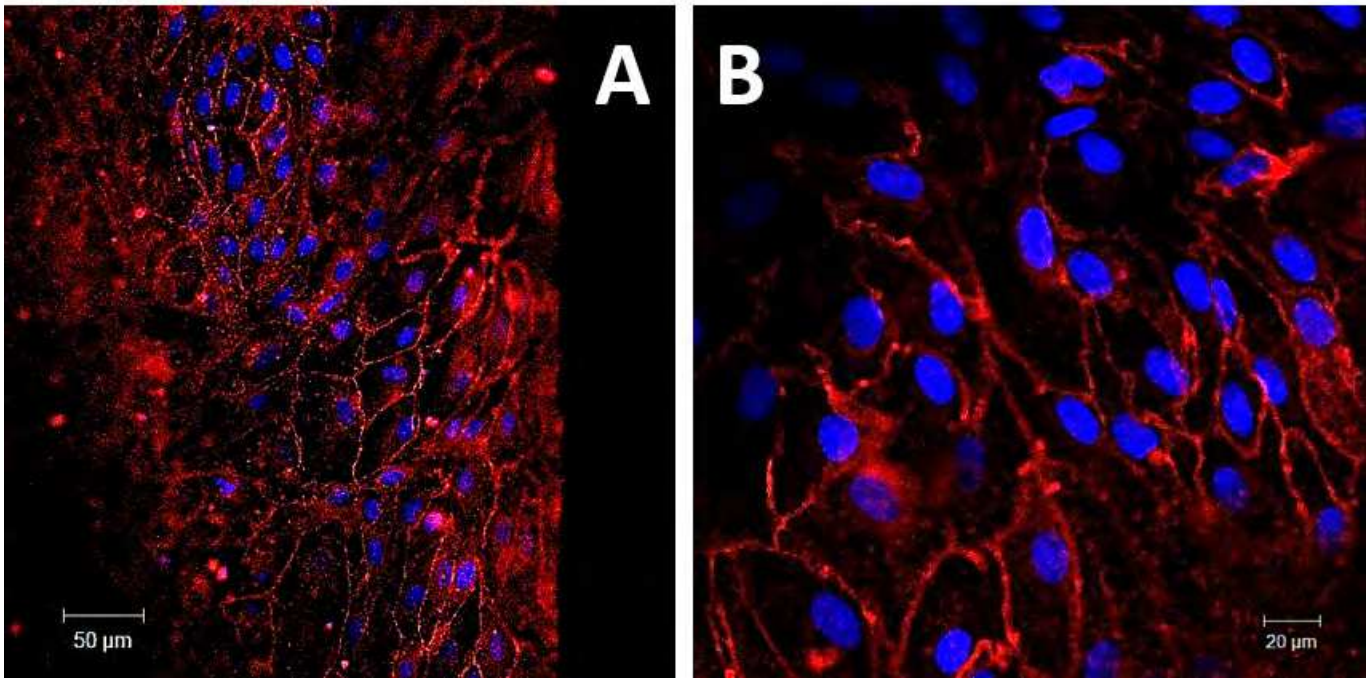

Figure 5

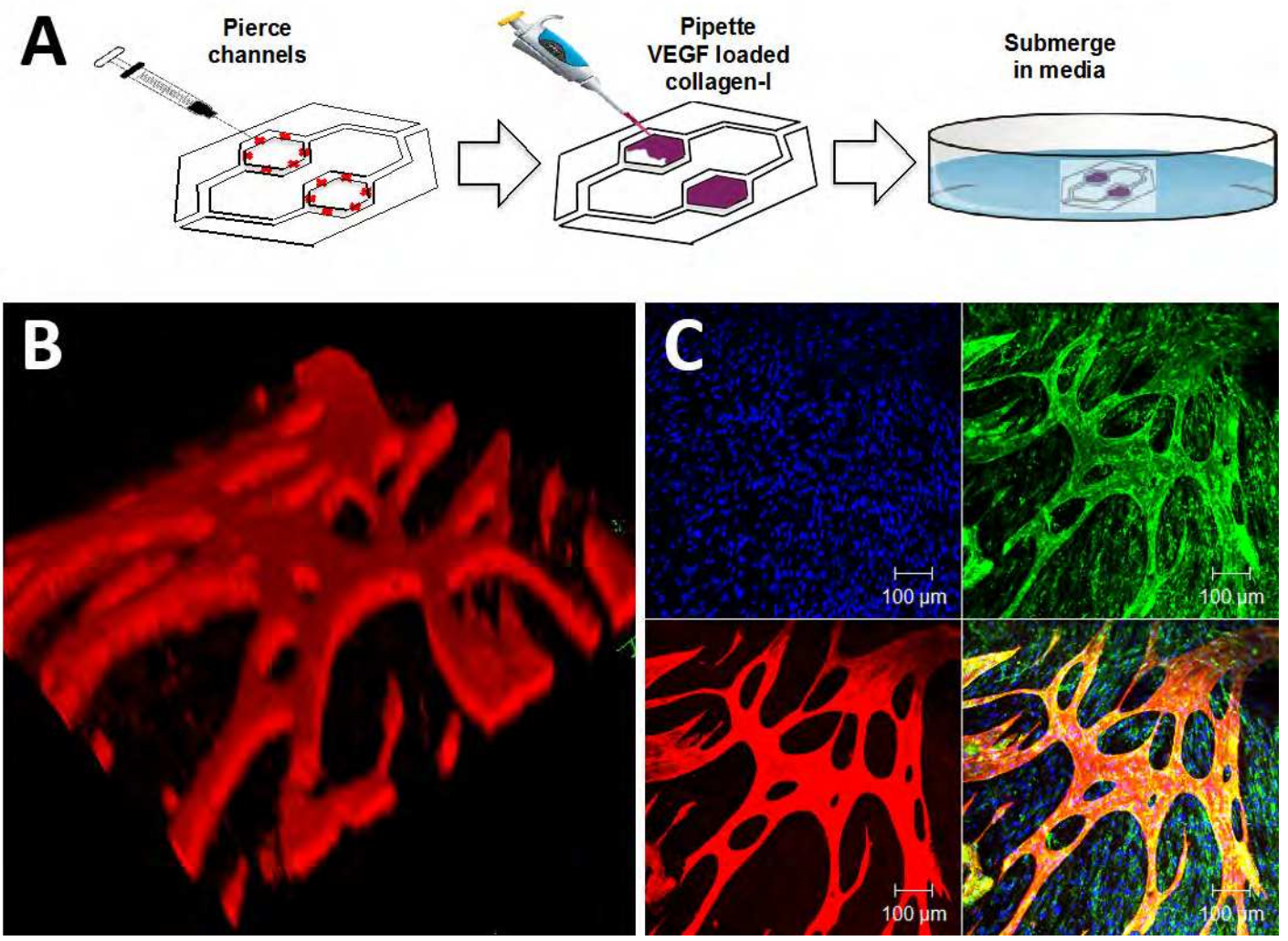
A
Pierce channels
Pipette VEGF loaded collagen-I
Submerge in media
B
C
100 µm
100 µm
100 µm
100 µm